Title

LEED SPOT PROFILE ANALYSIS OF THE STRUCTURE OF ELECTROCHEMICALLY TREATED Pt(100) AND (111) SURFACES

Author

Ross, P.N.

Publication Date

1984-09-01

LBL-18498
Preprint

Lawrence Berkeley Laboratory
UNIVERSITY OF CALIFORNIA

Materials & Molecular Research Division

Submitted to Surface Science

LEED SPOT PROFILE ANALYSIS OF THE STRUCTURE OF ELECTROCHEMICALLY TREATED Pt(100) AND (111) SURFACES

F.T. Wagner and P.N. Ross, Jr.

September 1984

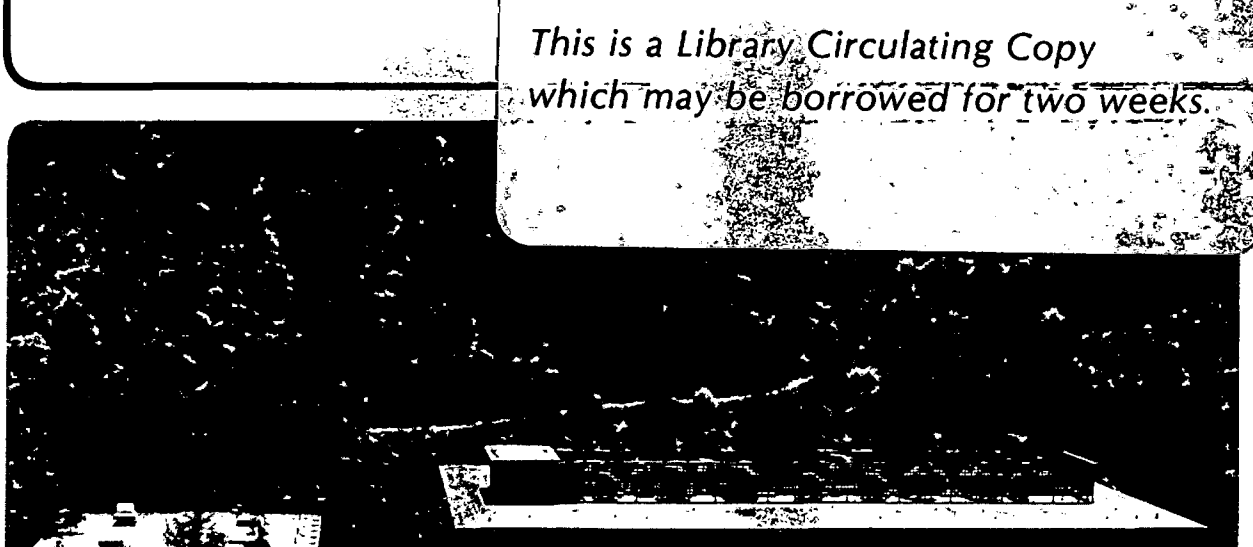

Prepared for the U.S. Department of Energy under Contract DE-AC03-76SF00098

DISCLAIMER

LEED SPOT PROFILE ANALYSIS OF THE STRUCTURE OF ELECTROCHEMICALLY TREATED PT(100) and (111) SURFACES

F.T. Wagner* and P.N. Ross, Jr.†

Materials and Molecular Research Division
Lawrence Berkeley Laboratory
Berkeley, CA 94720

†To whom correspondence should be addressed.

*Present Address: Physical Chemistry Department
General Motors Research Laboratories
Warren, MI 4809

ABSTRACT

The structures formed by oxidation-reduction cycling of ordered Pt (100) and (111) surfaces in aqueous electrolytes were studied using LEED spot profile analysis. Surfaces cycled to anodic potential limits above 1.0V(RHE) and emersed at 0.5V gave LEED spots which varied in width periodically with beam energy. The varying spot widths indicated a type of randomly stepped surface, and mean terrace widths were estimated by comparison with the previously published scattering calculations of Henzler and Lu and Legally. LEED spots from surfaces cycled to potentials below 1.0V(RHE) remained sharp at all beam energies. The restructuring resulted from the anodic formation of an amorphous surface oxide phase involving place exchange of platinum and oxygen followed by a reduction process in which the platinum atoms do not return to their original positions in the surface lattice. The observed spot profiles changed both the the number of cycles and with the upper potential limit. Cycling to 1.28-1.58V produced characteristically different structures than cycling to limits of 1.08 - 1.28V. At the higher potentials, a randomly-stepped surface was formed whose mean terrace width and extent of vertical relief were functions of the total anodic charge. Cycling to the lower potential limits produced a type of structure which is intermediate between the classical two-level island and the multi-level randomly-stepped structure. A three-level structure with a high degree of correlation between the first (island-like) and third (hole-like) levels is proposed for the latter.

1. Introduction

It has long been recognized that electrochemical oxidation- reduction cycling can modify the structure of Pt electrode surfaces [3-6], but direct structural techniques capable of characterizing these modifications at the atomic scale have been lacking. Recent experimental advances allowing the clean transfer of electrodes between ultra-high vacuum and high-purity electrochemical cells have enabled the application of LEED to surfaces produced electrochemically [7]. In the same time period the development of theory for LEED analysis of imperfect structures has proceeded to the point where cautious quantification of defect densities is possible [1,2,8,9]. In the present work, LEED patterns and spot profile data have been gathered for Pt(100) and Pt(111) surfaces cycled over specified potential regions in aqueous electrolytes. Analysis of the variation of the LEED spot profiles with beam energy and with electrochemical treatment has allowed the development of a statistical image of the real-space evolution of redox-cycled Pt surfaces. The results show that electrochemical cycling up to 1.0V RHE, within the normal operating range of oxygen-reduction electrodes for metal-air batteries of fuel cells, causes no LEED-detectable roughening of single- crystal Pt surfaces. However, excursions to higher potentials, followed by reduction, induce the formation of monatomic-height up-and-down steps with a moderately broad distribution of terrace widths in all crystallographic directions, leading to a "random mesa" structure. The structural modifications are linked to the formation of a thin disordered anodic layer and its quasi-epitaxial reduction.

Most of our knowledge of the interfacial electrochemistry of noble metals has been gleaned from electrodes cleaned of impurities by extensive

oxidation-reduction cycling. As long as polycrystalline electrodes were employed, the structural effects of this treatment were of minor concern. However, in recent work seeking to explore site-specific aspects of electrocatalysis and electrodeposition through the use of single-crystal electrodes [10-12], knowledge of the structural effects of such redox cycling is critical to proper interpretation of the data. The present work identifies the types of surfaces produced from Pt single crystals by a variety of electrochemical treatments.

LEED defect theory, after an initial burst of pessimism which arose from works showing the substantial deviations from perfection in surface order produced no readily apparent changes in LEED patterns [13-14], has advanced in two directions: 1) improvement of instrumentation so that smaller deviations from perfections can be detected [15]; 2) kinematic calculations of diffraction spot profiles for model surfaces with relatively high defect concentrations so that diffraction effects can be measured with standard instruments [1,2]. The latter direction is that most relevant to the present work. First-order approximations to the expected diffraction patterns for imperfect surfaces can be obtained through incoherent addition of diffracted intensity from many small patches, each of which is perfectly ordered. Such an approach is proper only if the patch size exceeds the coherence width, but it is readily tractable and provides useful insights into the qualitative diffraction behavior of more general random surfaces. The LEED behavior of perfectly ordered ascending step arrays is well understood [16]; Ewald constructions depicting the expected behavior of the (00), (10), (20), and (11) spots are given in Fig. 1 for ordered monatomic ascending steps running along the a) <010> and b) <011> directions of a Pt(100) surface. When the Ewald

circle passes through an intersection of the lattice rods due to the atom spacing within the terrace and the rods due to step spacing, a single sharp spot is observed, while at other energies sharp split spots are seen. For monatomic steps the relationship between the slope and spacing of the reciprocal lattice rods due to the steps is such that rods due to all possible terrace widths (quantized in atoms) intersect the atom-spacing rods at the same points, shown darkened in Fig. 1. For a surface with monatomic steps but a distribution of terrace widths sharp spots will still be seen at these beam energies; at other energies a large number of split spots with different separations will add incoherently to produce a broadened spot. For uniformly ascending steps this spot will be asymmetric about the extrapolated sharp spot position except exactly at out-of-phase energies (halfway in k-space between sharp spots). Equal numbers of up and down steps would remove this asymmetry, and steps in all crystallographic directions would produce broad spots with rotational symmetry about the spot centers. In several review papers [8,9,17] the results of the incoherent addition approach for a number of different defect types are summarized as Ewald constructions with beam-energy dependent thicknesses of the atom-spacing reciprocal lattice rods. Though the incoherent addition approach is useful in visualizing to first order the qualitative features of diffraction patterns from defect-containing surfaces, more quantitative analysis requires techniques which acknowledge the presence of different periodicities within distances smaller than the coherence width. To date only one-dimensional calculations of this type have been published; but when the spot profiles show no azimuthal dependence, as in this work, the one-dimensional results can be generalized to all directions. Two kinematic calculations of spot profiles taking the Fourier transforms of exact pair

correlation functions derived from model terrace width distributions have been published [1,2]; these provide the basis for comparison with the experimental data for electrochemically cycled surfaces in section 3.

2. Experimental

The electrochemical-UHV transfer system used in these studies has been described in detail elsewhere [7]. In brief, clean ordered Pt(100) and (111) surfaces were prepared by argon ion sputtering followed by ~ 10 min. annealing up to 850K in vacuum or 10^{-8} torr O_2. Surface cleanliness and order were verified with AES and LEED, the latter using standard Varian four-grid optics with off-axis electron gun. The crystal was moved to a transfer chamber which was then backfilled to slightly below one atmosphere with electronic-grade Ar further purified by pasing over Ti sponge at 1200K. The crystal was held at an electrochemical potential of +0.5V RHE while contact was made with an ~100μl droplet of electrolyte previously placed on the Pt ring - Pd disc counter-reference electrode assembly. Potentials were measured against the α-Pd reference electrode formed by previous electrochemical charging of the Pd disc with hydrogen; in acid electrolytes this electrode took on a potential of +0.075-0.085V vs. the reversible hydrogen electrode in the same electrolyte (RHE). All potentials are reported vs. RHE. The crystal was cycled first to the lower potential limit of 0.02V (in the hydrogen electrosorption region), then to the upper limit and back again a given number of times. The final negative-going potential sweep was stopped at ca. 0.05V, and the electrolyte was drained evenly out from between the crystal and the counter-reference electrode assembly through a polytetrafluoroethylene (PTFE) capillary. After

the transfer chamber was evacuated using sorption and turbomolecular pumps, the crystal was transferred back to the main UHV chamber for LEED analysis.

LEED patterns were photographed using 35mm Kodak Tri-X film, a 50mm lens with a +1 diopter close-up attachment, and an exposure of 30 s at f4. The LEED gun was operated in the constant filament voltage mode, set to give 1.0 Å current at a beam energy of 176eV; the current dropped with beam energy, reaching 0.2 A at 55eV. Beam profiles were obtained by scanning the negatives with a photometric microscope featuring a flexible fiber-optic probe which could be swept linearly across the field of vision. The photomultiplier output from the probe, which was proportional to the transmittance of a given point on the negative, was correlated with a reaching of the linear position sensor on the probe and stored on a floppy disc using an LSI 11/23-based minicomputer system. The transmittance (T) vs. position data were converted to intensity (I) readings through the relation $I = T^{-1.33}$.

Electrolytes were prepared using Harleco ultra-pure water (#64112) and electronics-grade reagents. They were further purified by 24h of galvanostatic Pt pre-electrolysis. The standard electrolyte was 0.3M HF prepared from Baker Ultretex-grade HF. This volatile electrolyte left detectable residue on the surface only when improper separation left visible droplets clinging to the electrode. Alternate non-volatile electrolytes 5×10^{-3} M H_2SO_4 (Baker Ultrex), 5×10^{-3}M NaOH (Apache ultra-pure 35% NaOH), and 5×10^{-4}M $NaHCO_3$ + 5×10^{-4}M Na_2CO_3 (Alpha Puratronic) left ~0.1 monolayer of nonvolatile residue on the Pt surface upon emersion of the electrode [18]. The electrodes were not rinsed with pure water before evacuation because such rinsing could not be done under potential control.

3. Results

Following the standard cleaning and annealing cycle for the Pt(100) crystal described in the previous section, the LEED pattern observed was not the (1x1) expected for a square lattice, but was one of a family of complex patterns frequently observed from a reconstructed surface. In particular, the clean, annealed surface consistantly produced the LEED pattern termed Pt(100)-hex by Heilman et al. [19a], as opposed to the other variations in the basically (1x5) patterns reviewed by Van Hove et al. [19b]. However, this surface was found to be unstable with respect to the electrochemical environment even in the absence of any applied potential. Transfer to the cell and contact even with pure water was observed to cause the conversion of the surface structure to (100) - (1x1). Adsorption of a small amount of CO during some stage of this experimental procedure may have been a factor in causing this transformation. In all the experimental results that are presented below, the effect of electrochemical oxidation and reduction on the surface structure is observed as a deviation in LEED patterns with respect to the (1x1) structure observed after contact with electrolyte in the absence of any applied potential.

3.1 Beam Energy Dependence of LEED Spot Widths- the Basic Phenomenon

Electrochemical oxidation of Pt(100) or (111) followed by separation from aqueous electrolytes at potentials above 1.1V produced anodic films which survived pumpdown and transfer to UHV. Studies of the composition and thickness of the anodic films comprise a separate paper [20]; however, to understand the

origin of the structural modifications to be considered here it is necessary to note that, at the highest electrode potential used in this study (1.58V RHE), the maximum charge going into anodic film formation per cycle was 550μC/cm^2 or 2.6e$^-$ per surface Pt atom. This corresponds to oxidation of 1.3 Pt atoms per surface site to the +II oxidation state or to the oxidation of 65% of the surface Pt atoms to the +IV state. Thus less than a bilayer of anodic film was formed and reduced during each cycle. The films appeared disordered to LEED; for potentials above 1.7V where near saturation coverages were achieved no LEED spots were visible. After partial oxidation at 1.2 - 1.7V only partially attenuated substrate spots and enhanced diffuse background were seen. Although the anodic films themselves were disordered, electrochemical reduction yielded Pt surfaces which gave LEED patterns with the characteristic variation of spot shape with beam energy which is the subject of this report.

Figure 2(a-c) compares the effects on Pt(100) LEED patterns of ten cycles in 0.3M HF between 0.02V (in the hydrogen adsorption region) and 0.82V (the edge of anodic film formation) or 1.58V (well into anodic film formation) followed by separation from the electrolyte at 0.4V (neither hydrogen nor oxygen adsorbed). In the 1.58V case all LEED spots alternated in width with changes in the indicent beam energy. At 176eV (Fig. 2a) the (10) and (20) spots were broad while the (11) spots were sharp. At 134eV (Fig. 2b) the (10) and (20) spots were sharp while the (11) spot was broad. At 114eV the (10) spot was broad, the (11) spot was sharp, and the (20) spot was off the screen. This alternation of spot width continued down to the beam energies where the spots left the screen and where the electron mean free path is at a minimum. In the 0.82V case no such modulation in spot width was seen. Comparison of these LEED patterns with the Ewald constructions of Fig. 1 shows that a given

LEED spot from the 1.58V cycled surface was sharp at the same incident beam energies where a single, sharp spot would be expected from a surface with ordered arrays of monatomic steps. These are the energies which satisfy the Bragg conditions for the three-dimensional crystal lattice; i.e. where in-phase scattering is obtained not only from scatterers in the surface mesh but also between consecutive planes parallel to the surface. The sharpness of these spots indicated that most of the surface atoms were in lattice positions of the three-dimensional crystal; the lack of sharpness at other energies shows that the surface atoms are not all in a single plane. For out-of-phase beam energies the redox cycled surfaces produced not the sharp split spots expected for an ordered stepped surface but broad spots with complex intensity vs. angle profiles. The sharp spots at in-phase energies and broader spots at out-of-phase energies are consistent with several defect structures: microfacets [8,9], random steps [1,2], and islands [21,22]. Facets on the order of the coherence width or larger can be ruled out because there was no indication of LEED intensity splitting off into specific directions towards discrete specular beams as the beam energy was slightly increased away from a Bragg energy. Distinction between LEED patterns due to random steps and to islands requires inspection of the profile shape as a function of beam energy, which will be undertaken in section 3.3. The LEED spots for cycled surfaces were broadened equally in all directions. This symmetry about the spot centers indicates an equal probability for step edges or islands in all directions; the "randomly stepped surface" is perhaps better visualized as a "random mesa structure".

The broad-sharp spot alternation after extensive cycling into the anodic film region was observed for all Pt surface/electrolyte combinations tried

including Pt(100): 0.3M HF (pH 2), $5x10^{3}$ M H_2SO_4 (pH 2), and $5x10^{-3}$M $NaHCO_3$ + $5x10^{-4}$M Na_2CO_3 (pH 10), and Pt(111): 0.3M HF, $5x10^{-3}$ H_2SO_4, and $5x10^{-3}$M NaOH. As before, cycling below the onset of anodic film formation caused no detectable LEED spot broadening. The type of structures produced on Pt by film formation and reduction thus seems general with regards to choice of low index plane and electrolyte. However, preliminary results showed that Pt(111) required cycling to somewhat higher potentials to produce LEED spot broadening equivalent to that seen on Pt(100).

Lightly Ar^+-sputtered Pt(111) also gave LEED spots which alternated in width with incident beam energy. As in previous studies of sputtered surfaces [23,23] the out-of-phase spot profiles showed single smooth intensity maxima rather than the more complex electrochemically generated spot profiles. The spot profiles for unannealed sputtered surfaces also showed greater breadth along the direction of the incident Ar^+ beam, while electrochemically broadened spots exhibited rotational symmetry.

Information about the distribution of step heights on a roughened surface can be obtained from the frequency components of a plot of spot width or spot splitting vs. beam energy. Such a plot for an extensively cycled Pt(111) electrode is shown in Fig. 3; similar behavior, though at different energies, was seen for cycled Pt(100). For an ordered stepped surface the spacing between the energies which produce sharp single spots gives the step height directly [25]. In the case of random steps, Lu and Legaly [2] have calculated spot width vs. beam energy relations corresponding to model surfaces having a given geometric terrace width distribution and various distributions of step heights. Comparison of the results of these calculations with the single, rather narrow maximum between the adjacent Bragg energies at 55 and 95eV in

Fig. 3 indicates that steps of monatomic height predominate on the electrochemically cycled surfaces. If mostly N-atom high steps were present one would expect N local maxima betwen 55 and 95eV. Even if the resolution of these maxima were lost due to experimental scatter or to a blurring of the high frequency effects by admixture of different step heights, the envelope of the curve for the multiple-height stepped surface would give a much broader maximum than that observed experimentally.

In contrast to the variation of LEED spot breadth with beam energy seen on Pt(111) cycled to 1.38V, LEED spots of near-constant width were obtained from Pt(111) cycled ten times between 0.02 and 0.83V (Figs. 3 and 4). This upper potential lies just above the unusual, highly reversible voltammetric peaks seen on well-ordered Pt(111) [7,26] but lies below the onset of irreversible anodic film formation. As shown in the left-hand photographs of Fig. 2, cycling Pt(100) to potentials below the onset of irreversible anodic film formation also had no effect on the LEED spot sharpness. The spot broadening after cycling to higher potentials is seen to be due to the formation and reduction of the disordered anodic film. Mere contact with the electrolyte or electrochemical cycling without formation of irreversible anodic films was not enough to produce detectable alteration of the surface structure, nor was hydrogen ad(ab)sorption/desorption cycling observed to structurally alter the Pt surface as suggested in earlier electrochemical work [27] .

Some diffuse background indicative either of a disordered adsorbate or of point defects was always seen in LEED patterns from electrochemically prepared surfaces, even those kept below the onset potential for anodic film formation. The same level of diffuse background and loss of the (100)-hex reconstruction of Pt(100) was seen on surfaces exposed only to backfill gases (argon and

electrolyte vapor). Auger electron spectroscopy showed that a small amount of carbon (equivalent to 0.1 layer of graphite by the calibration of Davis et al. [28]) was picked up at this point in the transfer operation. Thermal desorption showed the presence of water, probably associated with the carbonaceous impurities, on unoxidized surfaces exposed to liquid electrolyte or electrolyte vapors. When the higher levels of carbon contamination discussed in our previous report [7] were decreased to the present levels by the addition of a titanium getter to the backfill argon line, the LEED diffuse background showed a parallel decrease, indicating that the majority of the diffuse background was due to impurities and associated water rather than to point defects. While this impurity background precluded any attempt at estimation of the number of point defects, it was not sufficiently strong to prevent the use of spot profile analysis.

3.2 Electrochemical Potential Dependence of Spot Broadening

Both the full width at half maximum (FWHM normalized to the spacing between adjacent spot centers at the given beam energy) and the shape of the LEED spot profiles changed when the upper potential limit of cycling and/or the number of cycles were altered. Figure 5 shows spot profiles and Fig. 6 LEED patterns for a number of surface treatments. The profile in Fig. 5 of the annealed surface (with CO adsorbed to suppress the (100)-hex reconstruction) has a normalized FWHM at the instrumental limit of 0.03 but shows broad low-intensity shoulders. These indicate that defects induced by previous cycling or Ar bombardment had not been completely removed by the sputtering/annealing treatment used to renew the surface after each experiment.

The real-space distance corresponding to the separation of the shoulders is 30Å. Ten cycles to 1.00V (10x100μC/cm^2 film-forming anodic charge) caused little change in the spot profile. Ten cycles to 1.08V (10x200μC/cm^2) produced a moderately intense broad doughnut or halo around a sharp central peak of reduced intensity. The k-space separation between the intensity maxima of the halo corresponds in real space to ~20Å, though the resolution of the peak is not good. Fourteen cycles to 1.28V (14x450μC/cm^2) further supressed the central peak, leaving a broader spot with a shallow intensity minimum in the center (see Fig. 6) and a splitting corresponding again to about 20Å. Ten cycles to 1.58V (10x530μC/cm^2) produced a broad spot with less well-developed structure than was seen after 10x1.28V. The severity of the LEED pattern modification thus increased with the upper potential limit, at least over the range of 1.00-1.28V. Ten cycles to 1.00V produced barely detectable changes in the LEED pattern although enough anodic charge passed (1000μC/cm^2) to oxidize each surface Pt atom an average of 1.2 times to the +IV state or 2.4 times to the +II state over the entire 10 cycles. When the anodic charge passed was doubled by increasing the upper limit (10x1.08V) significant spot broadening occurred, but the continued presence of the sharp central peak at out-of-phase energies indicated that significant in-plane correlations remained. The central peak intensity was reduced to ~ 40% of its value for the annealed surface, suggesting that an average of one out of every four Pt oxidations to +IV or eight oxidations to +II was effective in shifting intensity out of the central spot. By 14x1.28V (5000μC/cm^2) the central peak could not be resolved.

3.3 Effects of Different Numbers of Cycles

The same total anodic charge could be obtained using fewer cycles to higher potentials or more cycles to lower potentials. One cycle to 1.58V (530 $\mu C/cm^2$) produced a pattern similar to 10x1.08V, but with more intensity left in the sharp central spot. The fact that a sweep with this much anodic charge left most of the LEED intensity in the central spot indicates an almost epitaxial reduction of the disordered anodic film, with a relatively small percentage of atoms going into atomic layers other than the original surface. Five cycles to 1.58V again produced a similar profile, but with more intensity shifted from the central spot than was seen for 10x1.08V. The severity of the LEED effects of 1x1.58V, 10x1.08V, and 5x1.58V thus followed the total anodic charges passed of 500, 2000, and 2700$\mu C/cm^2$, respectively. Over this potential region (1.08 to 1.58V) the total anodic charge passed, rather than the upper potential limit or number of cycles, appears to exert predominant control over the resulting structure.

Comparison of the results for 1,5, and 10 cycles to 1.58V indicated the progressive roughening of the surface with additional cycles. Experiments were performed with 100 cycles to explore two questions: (1) does the addition of defects continue with extended cycling to produce a totally disordered surface, or does an approximately steady-state surface result; (2) are changes in LEED spot profiles detectable after extended cycling to potentials lower than those required to produce discernable changes after ten cycles? LEED patterns taken after 100 cycles to 1.28 or 1.58V (33,000 or 50,000$\mu C/cm^2$) still gave sharp spots at in-phase beam energies although all spots showed reduced intensities. Out-of-phase energies gave halo spots similar in overall width to those for

14x1.28V but with a broader, more pronounced minimum in the center suggestive of the presence of fewer of the broader terraces. Since the changes in the LEED pattern were relatively minor it does appear that something like a steady-state surface (as regards local order) was reached after 5000$\mu C/cm^2$. After this point the real-space surface probably changed but the statistical distribution of LEED-detectable features was relatively unaffected. Kinoshita et. al. [6] have shown that extensive cycling (thousands of cycles) of polycrystalline Pt induced roughness on a much larger scale, visible by eye. This is not inconsistent with the LEED results, since the limited coherence width of the conventional LEED electron beam (~100Å) makes the technique insensitive to large-scale roughness.

Extensive cycling of Pt(100) to potentials below 1.28V generated LEED patterns which could not be produced at the higher potentials. While 10 cycles to 1.00V (1000$\mu C/cm^2$) produced a barely measurable shifting of intensity to the wings of the profiles (Fig. 4), 100 cycles (10,000$\mu C/cm^2$) depressed the central peak below the wings, yielding halo-type spots with smaller diameters than those produced by 14x1.28V (4600$\mu C/cm^2$). The normalized separation between the two intensity maxima in the profiles (i.e. halo diameters) appeared to vary continuously with beam energy (Fig. 7) in contrast to the constant normalized separations which have been reported for halo-type spots from island structures produced by vapor-phase epitaxy of tungsten [21] and silicon [22]. Although the total charge passed in anodic oxidation in this experiment was greater than that for the 10 cycle experiment at 1.58V, narrower out-of-phase LEED profiles resulted. Thus, the LEED spot profiles were not unique functions of oxidative charge over the entire potential range of anodization; more roughening per electron was obtained at 1.08, 1.28, and 1.58V than at 1.00V, and larger

average terrace widths were obtained at the lowest potential. 100 cycles to 0.90V (4200μC/cm^2) produced no broadening of the LEED spots beyond the residual effects which could not be annealed out, while 10x1.08V had produced definite broadening at 2000 C/cm^2. Two types of charge seemed to be associated with anodic film formation on Pt(100) in 0.3M HF: charge passed at potentials less than 1.0V, which had no effect on the surface structure; and charge passed above 1.0V, which produced LEED effects which correlated with anodic charge. At 1.0V a borderline condition occurred, with only a part of the charge leading to surface reconstruction. The likely chemical species associated with these types of charge will be discussed later, along with a comparison between these results and those from earlier, purely electrochemical, studies.

3.4 Spot Profile Shaped and Terrace Width Distributions

The preceeding sections have established that the Pt surface roughening induced by redox cycling belongs to a general class of defects in which atoms occupy lattice positions of the three-dimensional crystal. The behavior of the spot shapes near the in-phase energies precludes domination of the surface by microfacets larger than the coherence width. Two types of defects remain which are consistent with the gross features of the spot broadening: randomly-spaced steps and surface islands. Details of the profile shapes will now be considered which allow some discrimination between these two defect types and allow estimates to be made of characteristic dimensions on the roughened surfaces. Since the spot profiles had rotational symmetry about the spot center, it should be kept in mind that the single-dimensional analyses discussed here should be applied to all azimuthal directions.

The LEED pattern of any elemental surface is calculated as the Fourier transform of the pair correlation function of the scattering atoms. The earliest such calculation for a randomly-stepped surface by Houston and Park [13] used an average correlation function method valid for relatively narrow terrace width distributions. More general calculations using exact correlation functions calculated from model terrace width distributions have followed from Henzler [1] and Lu and Legally [2]. The Henzler calculation showed that random admixture of equal numbers of terraces with two different widths yielded a pair of rather narrow spots whose separation corresponded to the average terrace width. Broadening the distribution of terrace widths broadened each spot of the split pair, but their separation remained characteristic of the mean terrace width over a range of the distribution for a given average terrace width caused a coalescence of the split pair towards the center position until, for a particular broad terrace width distribution, the calculated spot profile emulated the nearly Gaussian profiles previously observed experimentally for ion-sputtered surfaces [23,24] . For this particular distribution a plot of out-of-phase spot HWHM vs. step density was developed. The algebraic form of the terrace width distributions used in the calculations was entirely artificial, chosen over others tested for its ability to predict the Gaussian profiles. Despite this origin, this form can also predict broad bimodal spot profiles of the type evident in Figs. 4 and 7 for extensively cycled surfaces. As will be seen, however, this model alone does not predict the spot profiles seen for lightly cycled surfaces.

3.4.1 Terrace Width Distributions for Extensively Cycled Surfaces

Extensively cycled surfaces defined as surfaces which have received >2000μC/cm^2 of anodic charge, gave spot profiles with either two intensity maxima or a broad, flat maximum suggestive of two unresolved peaks. As shown in Figs. 4 and 7 the normalized separation between the intensity maxima varied smoothly with beam energy following the pattern expected for a stepped surface as opposed to an array of islands. The observed profiles seem consistent with Henzler's calculations for randomly stepped surfaces with terrace width distributions somewhat narrower than those required to produce Gaussian profiles. If the normalized separation between the intensity maxima for out-of-phase beam energies is considered characteristic of the mean terrace width, Fig. 7 at 80eV implied mean terrace widths on Pt(100) of 7 atoms or 19Å for 100x1.0V and 5 atoms or 14Å for 100x1.28V. Similar treatment of the Pt(111) data of Fig. 4 gives a mean terrace width of 7 atoms or 20Å for 10x1.38V. Since the observed spot profiles most closely resemble Henzler's calculated calculated profile for a terrace width distribution for which the separation of the intensity maxima was 10-20% smaller than the reciprocal of the mean terrace width [2], these estimates are probably 10-20% high.

A separate set of diffraction calculations for randomly stepped surfaces has been performed by Lu and Legally [2]. While Henzler's empirically-fit terrace width distributions, $P(\Gamma)$, which peak about halfway between one atom and the mean terrace width, imply some repulsions between steps, Lu and Legally started with the expressed assumption of no step-step interactions. This assumption led to geometric terrace width distributions peaked at a terrace

width of one atom. The diffraction calculations based on this distribution produced single-peaked Lorentzian spot profile shapes which are at odds with the observed profiles for electrochemically cycled surfaces. Extrapolation of the FWHM vs. average terrace width relation for monatomic steps derived from this calculation led to the following mean terrace widths for electrochemically cycled surfaces: Pt(100) 100x1.00V, 4 atoms; Pt(100) 100x1.28V, 2.5 atoms; and Pt(111) 10x1.38V, 4 atoms. These mean terrace widths are lower than those derived using either method from Henzler's calculations. Figure 8 compares the geometric and Henzler's terrace width distributions $P(\Gamma)$ (not $P'(\Gamma)$) for Pt(100) 100x1.0V or Pt(111) 10x1.38V implied by the use of the mean terrace width vs. spot width or maxima separation relations for the two calculations discussed. While calculation of the geometric (or approximate geometric distribution) distributions, in which only the inverse of the mean terrace width is an adjustable parameter, was straight-forward, estimation of the appropriate Henzlerian distribution, which involves two adjustable parameters with no clear physical meaning, was less direct. The distribution shown was derived by finding the W which duplicated the published [1] Gausian profile using the quoted E=0.8, then increasing E to 1.0 to sharpen up the distribution by about the same amount which had been required to give two resolved intensity maxima for a mean terrace width of 10 atoms. The resulting profile (E=1.0, W=4) gives an average terrace of 6 atoms, 15% smaller than the 7 atoms estimated from the intensity maxima separation. Henzler's $P(\Gamma)$ distribution describes a surface with much less roughening than that implied by the geometric distribution. Since Henzler's calculations could reproduce the observed spot profile shapes for extensively cycled surfaces while Lu and Legally's did not, the Henzler's $P(\Gamma)$ distribution probably more accurately

describes the real-space condition of our surfaces.

In the case of the randomly-stepped type of surface structure, a unique transformation from reciprocal- space to real- space structure is not possible, and there can be a practically uncountable number of real- space structures that have equivalent features in reciprocal- space. The real- space physical structures that result from oxidation-reduction cycling are, therefore, difficult to represent in terms of a physical model, due both to the statistical nature of the mathematical description of the structure and to the complexity of the structure itself. The lower panel in Fig. 8 gives a model cross-section for a randomly up-down stepped surface with only monatomic steps and constant terrace width. The vertical axis is atomic displacement normal to the surface (zero indicating the position of all atoms in the surface prior to oxidation reduction cycling) and the horizontal axis is a direction parallel to the surface. The striking feature apparent in even this relatively simple up-down stepped surface is the large degree of vertical relief in the surface, where over a domain 50 terraces wide 8 different atomic layers are part of the surface. Within smaller domains of 4-5 terraces in size only three different levels are part of the surface, so that very large domains sizes are required to accurately represent all the features that these randomly up-down stepped surfaces possess. Such large domain sizes make physical models of the surface impractical, and one must be satisfied with a more abstract representation of the structure.

3.4.2 Mildly Cycled Surfaces

Pt(100) or (111) given a mild cycling treatment, e.g. total anodic charge

$<2000\mu C/cm^2$, produced spots with sharp centers and broad diffuse wings exemplified by the 10x1.08V profile in Fig. 5. Such halo plus spike profiles are not expected in the diffraction from a homogeneous, randomly stepped surface. Similarly-shaped spot profiles have been reported for W on W(110)[21] and Si on Si(111) [22] and have been ascribed to the formation of islands on a flat surface during vapor-phase epitaxy. Distances corresponding to the diameters of the islands of the inter-island spacings can produce the Fourier components responsible for the intensity of the wings of the profile [21]. However, the normalized separation of the wing maxima caused by such islands should be independent of the beam energy. This did not appear to be the case for the electrochemically cycled surfaces. Thus neither the island model nor the random step model adequately describes all features of the experimental results for this condition of cycling.

Because no single previously developed model for a homogeneous surface accurately predicts both the profile shapes and beam energy dependences found for mildly cycled surfaces, it is useful to consider whether the halo+central spot profiles could result from incoherent addition of intensities from roughened and unroughened patches larger than the coherence width of the electron beam. This would produce, in effect, two separate but superimposed LEED patterns; one from the smooth (never-oxidized) patches and one from the rough (redox-cycled) patches. If the central spot intensity arose only from never-oxidized regions of the surface, and if there were no correlation between the areas oxidized on successive cycles, the falloff in central intensity with successive cycles would be much more rapid than observed. If the oxidized areas were partially correlated on successive cycles the falloff in central intensity would be less rapid. However, in this case the same amount of charge

would decrease the central intensity more if passed as one cycle to high potential than as many cycles to lower potentials. This did not appear to be the case for anodic limits of 1.0x1.58V. Although never-oxidized areas do not seem possible as the source of the central intensity, Monte Carlo calculations have shown that statistical fluctuations in roughening processes uniformly applied to the surface without correlation between oxidized areas on consecutive cycles can still leave predominantly flat patches larger than the coherence width. The central peak need not arise from never-oxidized areas, but could originate from areas which have been oxidation-reduction cycled and remain flat due to the quasi-expitaxial nature of the reduction process.

Given the thinness of the anodic films, it is not surprising that the observed spot profiles for mildly cycled surfaces deviate from those expected for randomly-stepped surfaces. Figure 8 shows a random up-or-down sequence of steps. The extensive vertical relief (here 8 atomic planes) and relatively long series of steps in one direction (here up to 5) exhibited by the random surface are unlikely to arise from a few cycles at room temperature involving the formation and reduction of anodic films one or at most two monolayers thick. Rather, the mildly cycled surface will be on the average much closer to the original smooth surface, leaving many in-plane correlations. Although the mildly cycled surface has limited vertical development, it must be at least a three-level system since removal of atoms to form the overlying level must produce holes in the original surface, and monatomic steps are known to predominate. A fair concentration of groups containing at least two consecutive steps in one direction must be present. The three-level nature of the system may explain the variation in the normalized separation of the profile wings with beam energy, a phenomenon contrary to previous experimental

observation and calculation for predominantly two-level island structures [21,22]. The mildly cycled surfaces appear to be intermediate between an island structure and a randomly stepped surface, i.e. a three-level system with residual in-plane correlations.

3.5 LEED Effects of Cathodic and Thermal Annealing

Oxidation-reduction cycling similar to that which produces the randomly stepped surfaces reported here is the standard technique by which electrochemists clean noble metal electrodes, e.g. 10 cycles to 1.58V. The technique has been applied to single-crystal surfaces used in electrocatalysis studies, and the danger of disordering the surface has been recognized. However, it has been asserted that the roughening induced by cycling can be annealed out, at least in the case of gold, by holding the electrode at reducing potentials [29]. This supposition was tested by LEED with the results for Pt(100) cycled 10x1.58V shown in Fig. 9. After the top LEED profile was taken, the crystal was transferred back to the electrochemical cell, cycled twice to remove any possible impurities picked up during transfer, and then held 15 min. at 0.06V (in the hydrogen electrosorption region). After pumpdown and transfer a (20) spot profile with the same reduced normalized halfwidth of 0.21 was seen; the only difference between the profiles for the freshly cycled 10x1.58V and the "cathodically annealed" cases was a slight reduction in central intensity for the latter, ascribable to the two extra cycles. Although cathodic "annealing" induced no changes in the LEED profiles, thermal annealing in vacuo caused pronounced sharpening of the (20) profile. Ten minutes at 500K decreased the reduced half-width to 0.13; a further ten minutes at 600K reduced

it to 0.07; and ten minutes further heating, reaching a maximum temperature of 850K, reduced it to the apparent minimum width at 176eV. The surfaces annealed at higher temperatures show some intensity away from the main spots due to the emergence of the (100)-hex reconstruction and a faint (2x2) structure or 2 domains of (2x1) which appeared when the carbon contamination picked up during backfill and pumpdown was annealed at high temperatures. Although cathodic holding at room temperature for times consistent with the maintenance of surface purity in even high-purity electrolytes seems ineffective in removing surface steps from Pt, annealing at relatively low elevated temperatures can significantly reduce the concentration of electrochemically-induced low-coordination sites. Electrochemical cycling at the elevated temperatures used in phosphoric acid fuel cells (~430K) could well produce surfaces considerably smoother than those reported here.

4. Discussion

4.1 Comparison with Previous Electrochemical Results

LEED showed spot shape variations with beam energy for Pt surfaces on which anodic films were repetitively formed at or above 1.0V RHE and then reduced. No such spot size variation was observed for surfaces subjected to hydrogen electrosorption/desorption cycling or for surfaces on which partial anodic films were formed below 1.0V. This difference in LEED behavior allows the distinction between two modes of "adsorption" of oxygenated species: (1) surface adsorption and (2) "adsorption" into a new surface phase. The former mode involves little if any displacement of platinum atoms from the bare,

well-ordered surface and repetitive surface adsorption/desorption cycling has no cumulative structural effect. The latter involves motion of Pt atoms out of their metallic surface mesh positions into a surface phase in which the Pt atomic density is different from that in the metal and in which some oxygen atoms lie below some Pt atoms. Upon reduction of such a phase the Pt atoms need not return to their original positions in the surface mesh, and cumulative structural effects may be seen.

The present LEED results are in general agreement with the picture of Pt anodization which has been built up over several decades of electrochemical experimentation. Cyclic voltammetry has shown that, while hydrogen adsorption and the initial stages of anodic film formation are electrochemically reversible, anodic films formed at higher potentials can be reduced only at potentials significantly lower than those at which they were formed. This irreversibility has been attributed to structural rearrangement involving motion of Pt atoms [30]. The growth kinetics of anodic films on noble metals have indicated a rate-determining step dependent upon the electric field strength at the metal-film or film-electrolyte interfaces [31,32]. Vetter and Schultze [31] have interpreted the source of this field dependence as the requirement for an electric field to drive the place exchange of Pt atoms and O or OH species, i.e. to allow the intermixing of Pt atoms and O species during the formation of a new phase. Angerstein-Kozlowska et al. (KCS) [33] have published a detailed interpretation of voltammetric and ellipsometric data on the anodization of polycrystalline Pt in aqueous sulfuric acid. They proposed the generation of surface adsorbed hydroxyl species over the potential interval 0.8 to 0.95V, in agreement with the present results in which anodic charge was passed over this potential region without causing LEED- detectable

restructuring in the cycled surfaces. Above 0.95V they found that irreversibility began in the form of a displacement of the reduction peak to lower potentials with increasing film-forming charge and ascribed the irreversibility above 1.0V to Pt-OH place exchange. The onset of LEED-detectable restructuring at 1.0V provides more direct physical confirmation of their conclusion drawn from electrochemical data. KCA found that films formed for varying times in the potential region 1.0-1.2V gave a constant reduction peak potential despite a range of 200-400$\mu C/cm^2$ in the total film-forming charge. They ascribed this constant peak potential to invariance of the place-exchanges Pt-O structure, assigning the 200$\mu C/cm^2$ of charge passed in this region to the oxidative deprotonation of previously place-exchanged hydroxyl groups, i.e. $PtOH \rightarrow PtO + H^+ + e^-$. This latter conclusion appears inconsistent with details of the LEED restructuring data for the films formed by continuous cycling at 100mV/s in our experiments. If the anodic charge passed in this region corresponded merely to oxidative deprotonation and not to additional place-exchange of OH with Pt, one would expect no additional step introduction to result from increasing the upper limit of cycling fromn 1.0 to 1.2V. The extent of LEED restructuring did increase over this potential range, suggesting that no constant-structure deprotonation of previously place-exchanged films occurred on the time scale of these experiments. Thermal desorption done in parallel with this LEED work [20] showed that all transferable films were hydrated to the extent of one water molecule per oxygen atom desorbing as O_2 (i.e. $PtO_x \cdot x\ H_2O$). Since the films formed at higher potentials were fully hydrated, the anodic charge pased in this range could not have simply removed protons without altering the Pt-O framework. The thermal desorption results from films formed at constant potential for two minutes thus

reinforce the conclusion drawn from LEED results for surfaces cyled at a constant 100mV/s. The constant reduction potential which led to the oxidative deprotonation proposal might arise from details of the shape and sizes of islands, and some of the aging phenomena previously ascribed to dehydration may also arise from island reorganization. The application of LEED spot profile analysis has provided direct physical evidence for some conclusions on structural transformation previously drawn indirectly through thoughtful analysis of electrochemical data. On the major points of place exchange good agreement has been found, but the surface analytical data does not support the earlier conclusions about the formation of anhydrous oxides.

KCS also proposed several different ordered states of surface-adsorbed hydroxyls to account for features in the anodic voltammetry below 1.1V. Unfortunately, these proposals could not be tested by LEED because the electrochemically reversible anodic films formed below 1.1V did not survive emersion and pumpdown. These films are likely to resemble the surface-adsorbed hydroxyl species formed in UHV by low-temperature sequential adsorption of oxygen and water vapor [34]. In the absence of an externally applied electric field, these species spontaneously decompose to water and adsorbed oxygen well below room temperature, and the adsorbed oxygen is notoriously reactive with species likely to be found in the background gases of UHV and transfer chambers.

4.2 Mechanism of Electrochemical Surface Restructuring

The electrochemical potential dependence of LEED spot profile broadening has given a direct structural determination of the onset of place exchange.

While it is clear that place exchange can produce vertical motion of Pt atoms, it is not immediately clear why the particular types of surfaces deduced from the LEED data in section 3 should result. The introduction of random steps has been observed for a number of other surface processes, including ion-sputtering [23,24] and chemical etching [35]. Although the random-step phenomenon, as evidenced by regular modulation of LEED spot widths with beam energy, thus appears rather general, the mechanism by which these steps are introduced is uniquely different in our case.

In the anodic place-exchange process, Pt atoms move out of their metallic lattice positions in order to accomodate more than a monolayer of oxygen species. The driving force for this process is the electrical potential gradient across the metal solution interface, which is being changed by an imposed bias. The particular oxygen species involved in place-exchange is not known by independent measurement, but the potential dependence and the charge dependence of the place-exchange process allow reasonable inferences to be made about the nature of these species. The critical potential for the anodic limit in cycling was 1.0V; below this potential no structural changes were observed even with many hundreds of cycles, and at 80mV above this potential reorganization of the surface was observed. Coulommetry indicated that the anodic charge accumulated in the critical potential region 1.0-1.08V was ca. 200-300 $\mu C/cm^2$, so that the critical amount of anodic charge is essentially equal to that for a monolayer of $1e^-$ oxygen species ($\cdot OH$), 220 $\mu C/cm$ for (100)-1x1 and 255 $\mu C/cm^2$ for (111). It is also possible that the critcal charge corresponds to half-monolayer of 2e species ($O\cdot H_2O$ or 2OH per Pt) via a patch-wise mechanism. The extent of vertical development of the surface with increasing charge seems to indicate that patch-wise place-exchange involving

$2e^-$ species was not the principal process, since a single cycle to an anodic charge of 550 $\mu C/cm^2$ produced vertical development involving place-exchange of at least two atomic layers. KCS in their study using purely electrochemical methods also concluded that the $1e^-$ oxygen species was the anionic species in the place-exchange process in this potential region.

Upon reduction, the displaced Pt atoms do not necessarily return to their original positions in the surface lattice, and cumulative structural changes occur and are what we observe by LEED. The physical structure that evolves from these oxidation-reduction processes clearly depends on a myriad of (possible) elementary steps, but it is not clear which of the many possible steps are important in establishing the structure. Some of the factors we consider important in these processes are: the selectivity of place-exchange, where the probability of displacement is greater at some sites than at others; reduction in place leaving adatoms and vacancies which migrate and nucleate into islands and holes, respectively; reductive dissolution of Pt and subsequent electrodeposition of dissolved Pt; adatom interactions; vacancy interactions; solution transport of dissolved Pt and site-selective electrodeposition of dissolved Pt. Using only LEED analysis of the structural evolution of the surface, we have, at best, a picture of the surface before and after these processes have occurred, and what happens in between can only be inferred from these pictures. We have initiated Monte-Carlo type modelling of some of the elementary steps mentioned, but this has not yet improved our understanding of structural evolution. Given the experimental difficulties in observing some of these intermediate processes individually, we plan to continue Monte-Carlo type calculations in order to define the key experiments for future study.

Although it is clear that place-exchange is the critical process that

initiates structural change, the evolution of the structure with repeated cycling depends on numerous companion physical processes that are not understood at present.

Conclusions

LEED spot profile analysis has shown that oxidation-reduction cycling of Pt(111) and (100) surfaces to potentials above 1.0V RHE in 0.3M HF electrolyte causes reorganization of the surface structure. While the mechanism of this surface reorganization is not completely understood, it is clear that the critical process leading to structural change is the place-exchange of Pt surface atoms during anodic oxidation. In this process, Pt surface atoms move out of their metallic positions in order to accomodate more than a monolayer of oxygen species. Upon reduction, the Pt atoms do not necessarily return to their original positions in the surface lattice, and cumulative structural effects occur and are what we observed by LEED. The extent of surface reorganization was found to depend on the anodic potential limit, the number of cycles, and the total amount of anodic charge passed during cycling. Above 1.08V, the critical amount of charge to produce a change in surface structure observable by LEED was ca. 500$\mu C/cm^2$. Cycling to anodic potential limits of 1.28-1.58V produced characteristically different structures than cycling to limits of 1.08-1.28V. At the higher potentials, the kinematic analysis indicates a randomly stepped surface was formed whose mean terrace width and extent of vertical relief were functions of the total anodic charge. Extended cycling indicated a steady-state surface structure was reached after ca. 5000 $\mu C/cm^2$ of total anodic charge. Cycling to the lower potential limits produced a type of structure intermediate between the classical two-level island (adatom) structure and a randomly-stepped structure, which we suggest is a three-level

structure with a high degree of correlation between the first (islands) and third (holes) levels. Although place-exchange is the critical process that initiates structural change, the evolution of the structure depends on numerous physical processes that accompany the place-exchange reaction, e.g. diffusion and nucleation of Pt adatoms, migration and nucleation of vacancies, solution transport of dissolved Pt, and deposition of dissolved Pt. These companion processes appear to play a dominant role in determining the type of surface structure that results from oxidation-reduction cycling.

Acknowledgments

This work was supported by the Assistant Secretary for Conservation and Renewable Energy, Office of Advanced Conservation Technology, Division of Electrochemical Systems Resources of the U.S. Department of Energy under Contract Number DE-AC03-76SF00098. PNR acknowledges valuable discussions with Max Legally and Martin Henzler during the preparation of this manuscript.

References

1. M. Henzler, Surf. Sci. 73 (1978) 240.
2. T.-M. Lu and M.G. Lagally, Surf. Sci. 120 (1982) 47.
3. S. Gilman, J. Electroanal. Chem. 9 (1965) 276.
4. F.G. Will, J. Electrochem. Soc. 112 (1965) 451.
5. T. Biegler, J. Electrochem. Soc. 114 (1967) 1261.
6. K. Kinoshita, J.T. Lundquist, and P. Stonehart, J. Electroanal. Chem., 48 (1973) 157.
7. F.T. Wagner and P.N. Ross, Jr., J. Electroanal. Chem. 150 (1983) 141; also P.N. Ross, Jr. and F.T. Wagner in H. Gerischer (ed.) Adv. in Electrochem. and Electrochem. Eng., Volume 13, J. Wiley and Sons, New York, 1984, pp. 69-112.
8. M. Henzler, Applic. Surf. Sci. 11 (1982) 450.
9. M.G. Lagally in R. Vanselow and R. Howe (ed.), Chemistry and Physics of Solid Surfaces IV, Springer Series in Chem. Phys. 20, Berlin, 1982, p. 281.
10. J.D.E. McIntyre and W.F. Peck, Jr., Electrochem. Soc., Extended Abstracts, 82-1 (1982) 1017.
11. R.R. Adzic, W.E. O'Grady, and S. Srinivasan, Surf. Sci., 94 (1980) L191.
12. C. Lamy, J.M. Leger, J. Clavilier, J. Electroanal. Chem., 135 (1982) 321.
13. J.E. Houston and R.L. Park, Surf. Sci. 26 (1971) 269.
14. F. Jona, Surf. Sci. 8 (1967) 57.

15. K.D. Gronwald and M. Henzler, Surf. Sci. 117 (1982) 180.

16. W.P. Ellis and R.L. Schwoebel, Surf. Sci. 11 (1968) 82.

17. M. Henzler in H. Ibach (ed.), Electron Spectroscopy for Surface Analysis, Topics in Current Physics, 4, Springer, Berlin, 1977, p. 117.

18. F.T. Wagner and P.N. Ross, Jr., J. Electrochem. Soc., 130 (1983) 1789.

19. (a) P. Heilmann, K. Heinz and K. Muller, Surf. Sci., 83 (1979) 487; (b) M. Van Hove, R. Koestner, P. Stair, J. Biberian, L. Kesmodel, I. Bartos, and G. Somorjai, Surf. Sci., 103 (1981) 189.

20. F.T. Wagner and P.N. Ross, Jr., submitted to Applications of Surf. Sci.

21. P. Hahn, J. Clabes, and M. Henzler, J. Appl. Phys.. 51 (1980) 2079.

22. K.D. Gronwald and M. Henzler, Surf. Sci., 117 (1982) 180.

23. G. Schultze and M. Henzler, Surf. Sci., 73 (1978) 553.

24. D.G. Welkie and M.G. Lagally, J. Vac. Sci. Technol., 16 (1979) 784.

25. K. Besocke and H. Wagner, Surf. Sci. 52 (1975) 653.

26. J. Clavilier, D. Armand, and B.L. Wu, J. Electroanal. Chem., 135 (1982) 159.

27. J.P. Hoare, HJ. Electroanal. Chem., 12 (1966) 260.

28. S.M. Davis, B.E. Gordon, M. Press and G.A. Somorjai, J. Vac. Sci. Technol., 19 (1982) 231.

29. D. Dickertmann, J.W. Schultze, and K.J. Vetter, J.

Electroanal. Chem., 55 (1974) 429.

30. D. Gilroy and B.E. Conway, Can. J. Chem., 46 (1968) 875.

31. K.J. Vetter and J.W. Schultze, J. Electroanal. Chem., 34 (1972) 131.

32. A. Ward, A. Damjanovic, E. Gray, and M. O'Jea, J. Electrochem. Soc., 123 (1976) 1599.

33. H. Angerstein-Kozlowska, B.E. Conway, and W.B.A. Sharp, J. Electroanal. Chem., 43 (1973) 9.

34. G.B. Fisher and B.A. Sexton, Phys. Rev. Lett., 44 (1980) 683.

35. M. Henzler and F.W. Wulfert, in F.G. Fumi, ed., Proc. XIII Intern. Conf. Phys. Semicond., Rome, 1976, p. 669.

36. D.C. Johnson, D.T. Napp, and S. Bruckenstein, Electrochimica Acta, 15 (1970) 1493.

37. D.W. Bassett and P.R. Webber, Surf. Sci., 70 (1978) 520.

Figure Captions

Fig. 1. Ewald constructions for ordered steps along (a) 010 and (b) 011 directions of a Pt(100) surface. Filled dots signify single sharp LEED spots; unfilled dots signify split spots.

Fig. 2. LEED patterns for Pt(100) separated from 0.3M HF at 0.4V RHE after ten cycles to: left, 0.82V; right, 1.58V. Beam energies (a) 176eV, (b) 134eV, (c) 114eV.

Fig. 3. Full width at half maximum of (01) LEED spot from Pt(111) (normalized to distance between adjacent LEED spots) vs. beam energy. Cycled as noted.

Fig. 4. (01) spot profiles for Pt(111), cycled as noted, between two consecutive Bragg energies.

Fig. 5. (11) spot profiles for Pt(100) at 76eV after a variety of surface treatments in 0.3M HF.

Fig. 6. Pt(100) LEED patterns at 176 eV after cycling in 0.3M HF: (a) 10x1.08V, (b) 14x1.28V, (c) 10x1.58V.

Fig. 7. (11) spot profiles for Pt(100) cycled in 0.3M HF: 10x0.82V, 100x1.0V, and 100x1.28V. Bragg energies are 60 and 110eV.

Fig. 8. (upper panel) Terrace width distributions corresponding to data for Pt(100) 100x1.00V or Pt(111) 10x1.38V using distribution functions of Henzler [1] and Lu and Lagally [2]. $P(\Gamma)$ is the probability that a given terrace will be Γ atoms wide. (lower panel) Vertical

development of a surface with random choice of up and down monatomic steps. Terrace size held constant for simplicity.

Fig. 9. (20) spot profiles at 176eV for Pt(100) 10x1.58V showing effects of cathodic hold and of thermal annealing.

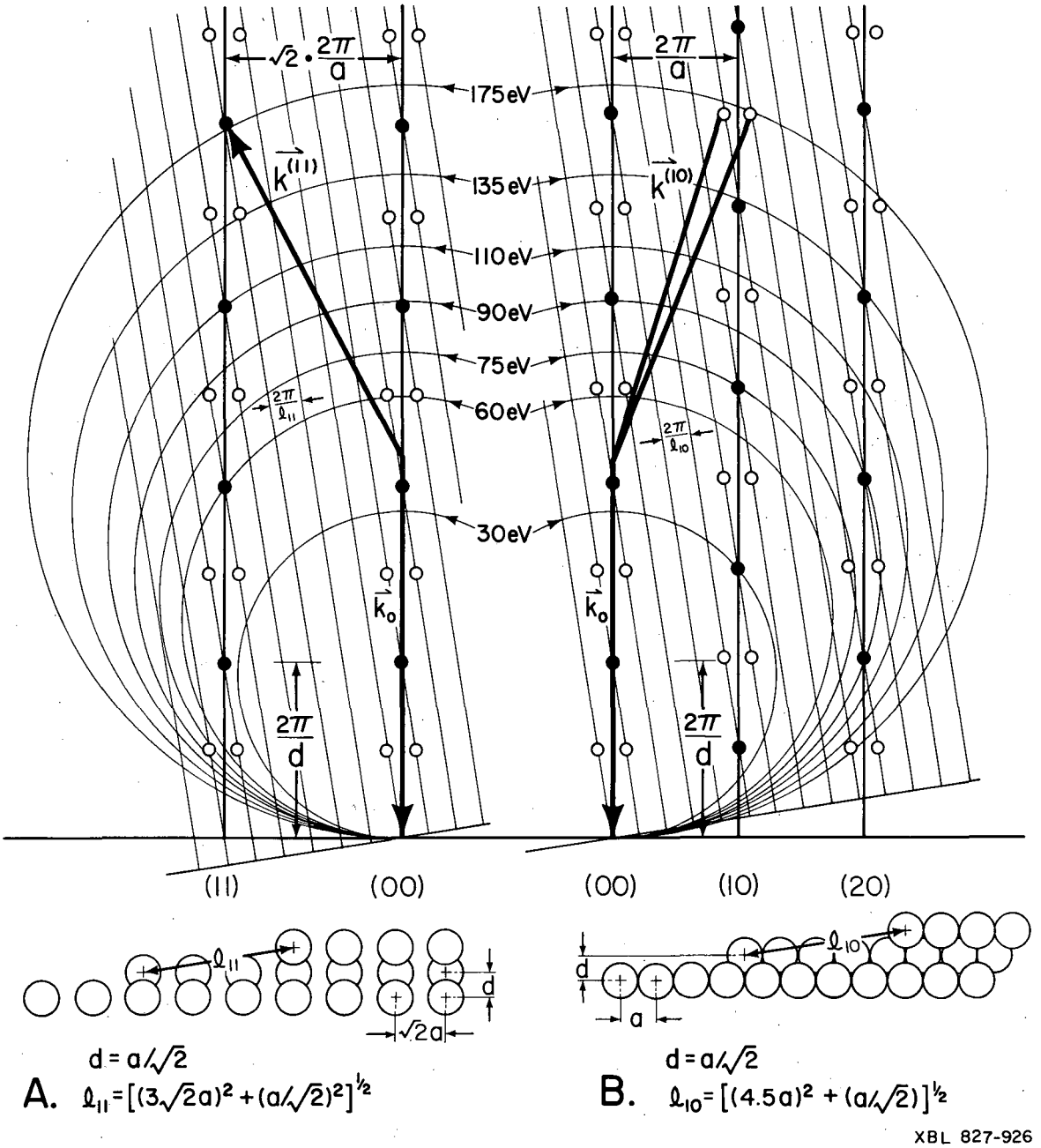
√2 · 2π/a
2π/a
175eV
135eV
110eV
90eV
75eV
60eV
30eV
k(11)
k(10)
k0
2π/d
2π/ℓ11
2π/ℓ10
(11)
(00)
(00)
(10)
(20)
ℓ11
d
√2a
ℓ10
a
d = a/√2
A. ℓ11 = [(3√2a)² + (a/√2)²]^½
d = a/√2
B. ℓ10 = [(4.5a)² + (a/√2)²]^½
XBL 827-926

Fig. 1

LEED 176 eV

after ten cycles

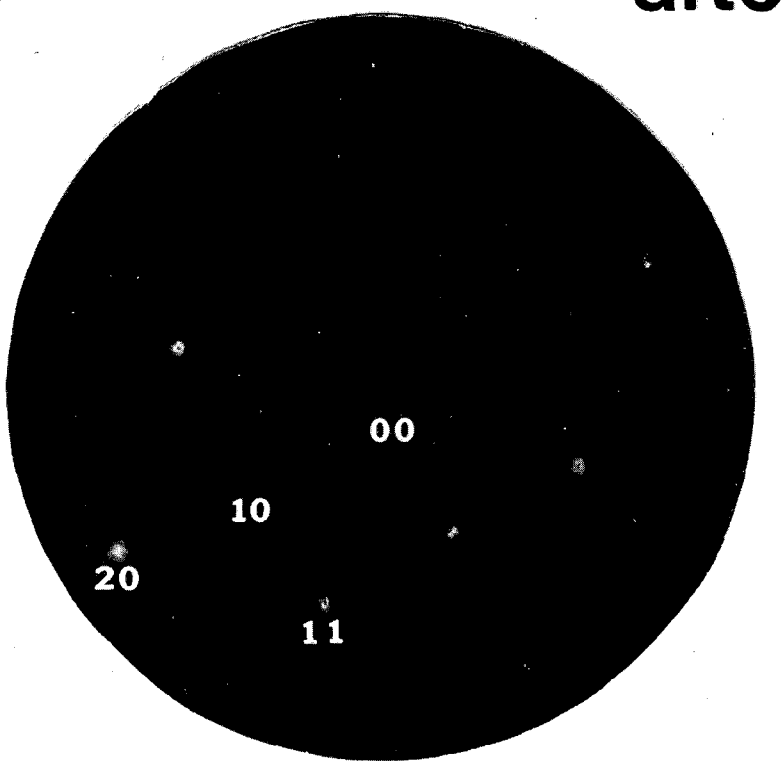

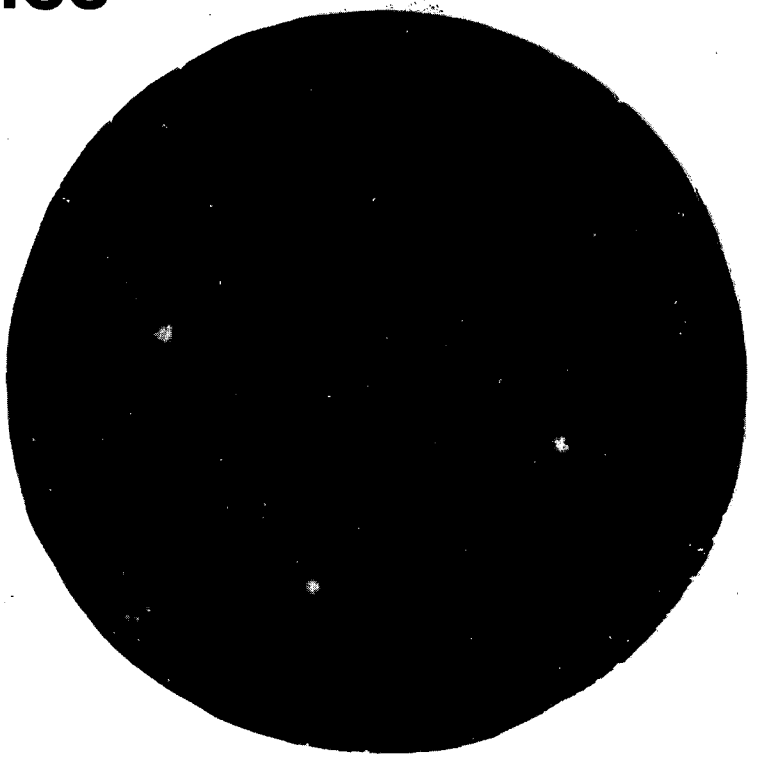

to 0.82 V (RHE)

to 1.58 V (RHE)

XBB834-3505

Fig. 2(a)

LEED 134 eV

after ten cycles

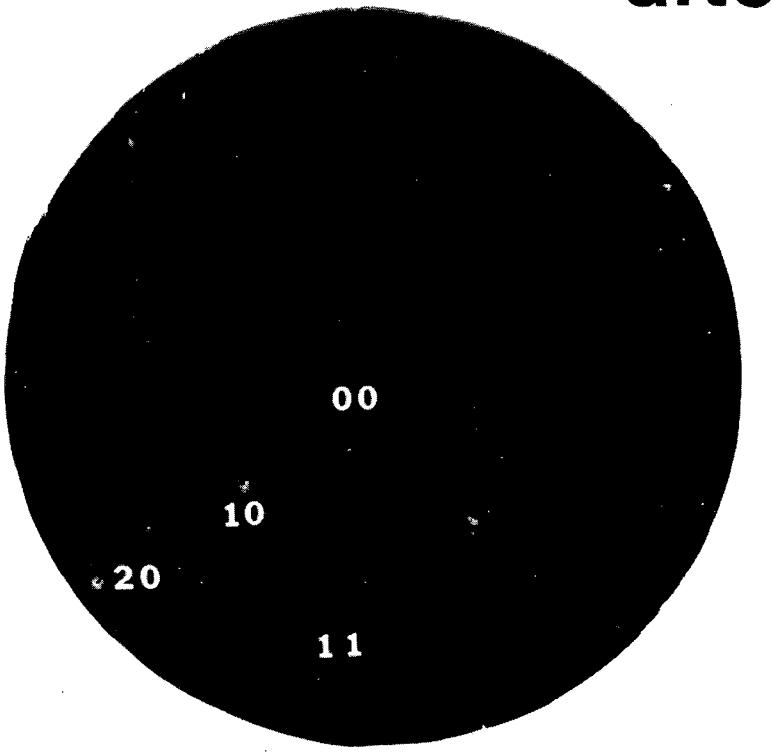

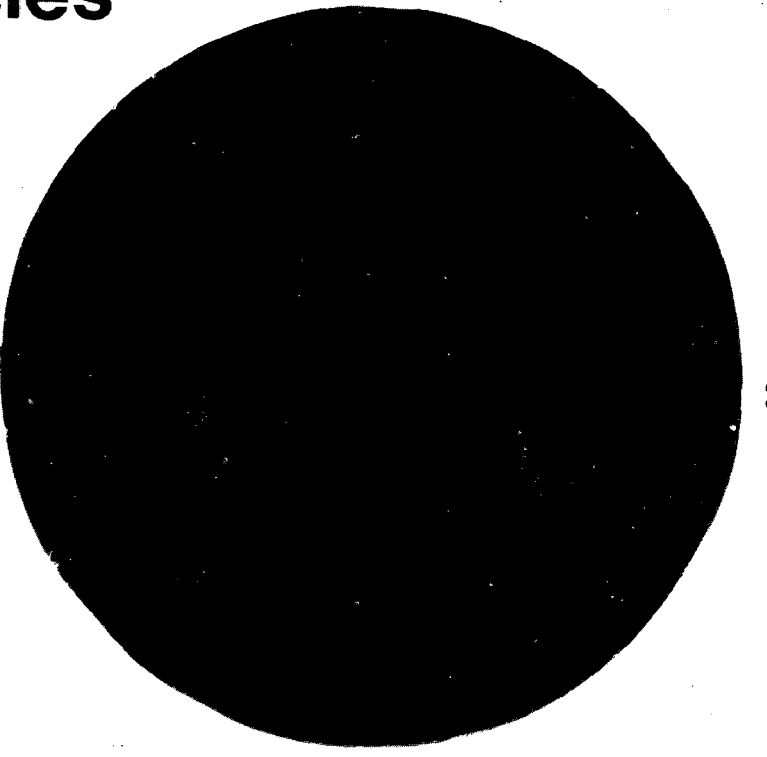

to 0.82 V (RHE)

to 1.58 V (RHE)

XBB 834-3504

Fig. 2(b)

LEED 114 eV
after ten cycles

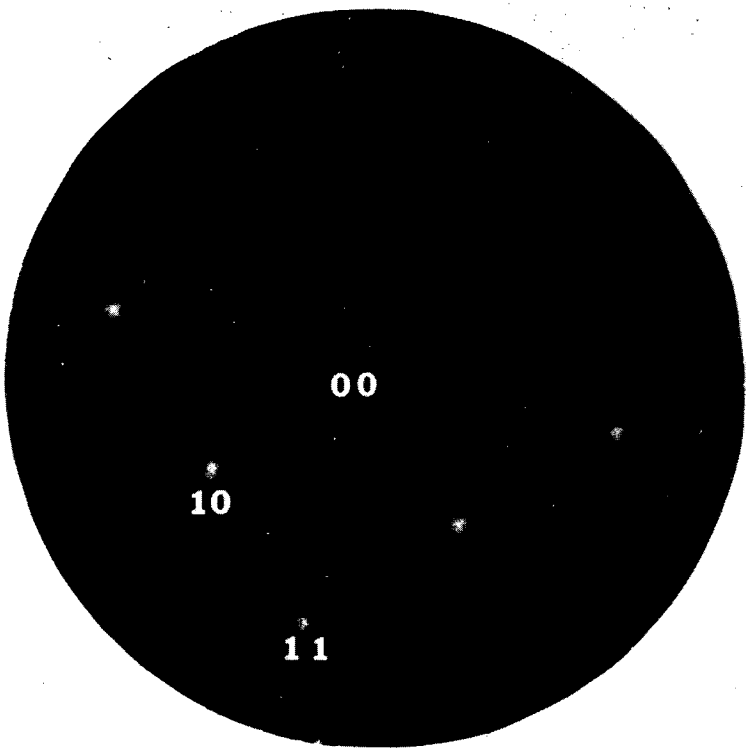

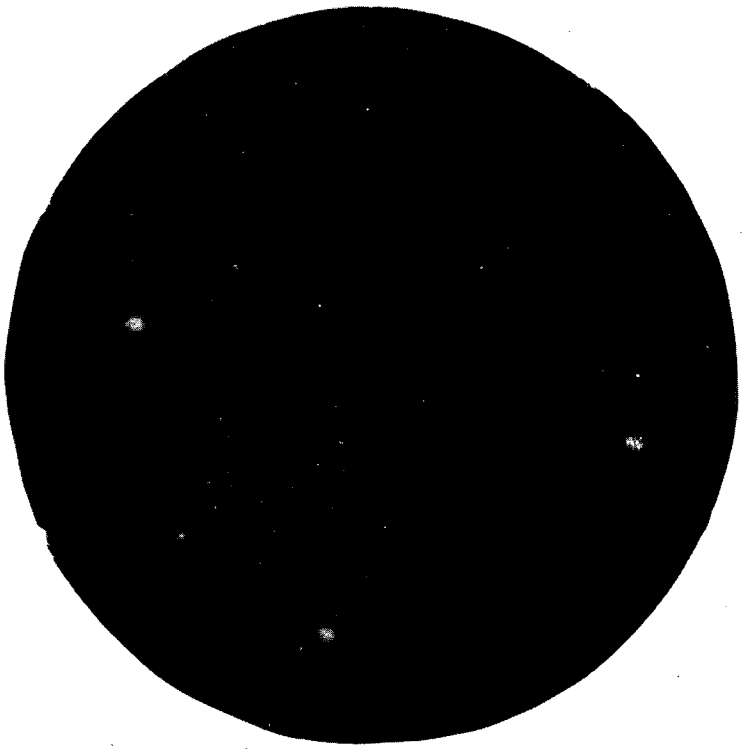

to 0.82 V (RHE)

to 1.58 V (RHE)

XBB 834-3503

Fig. 2(c)

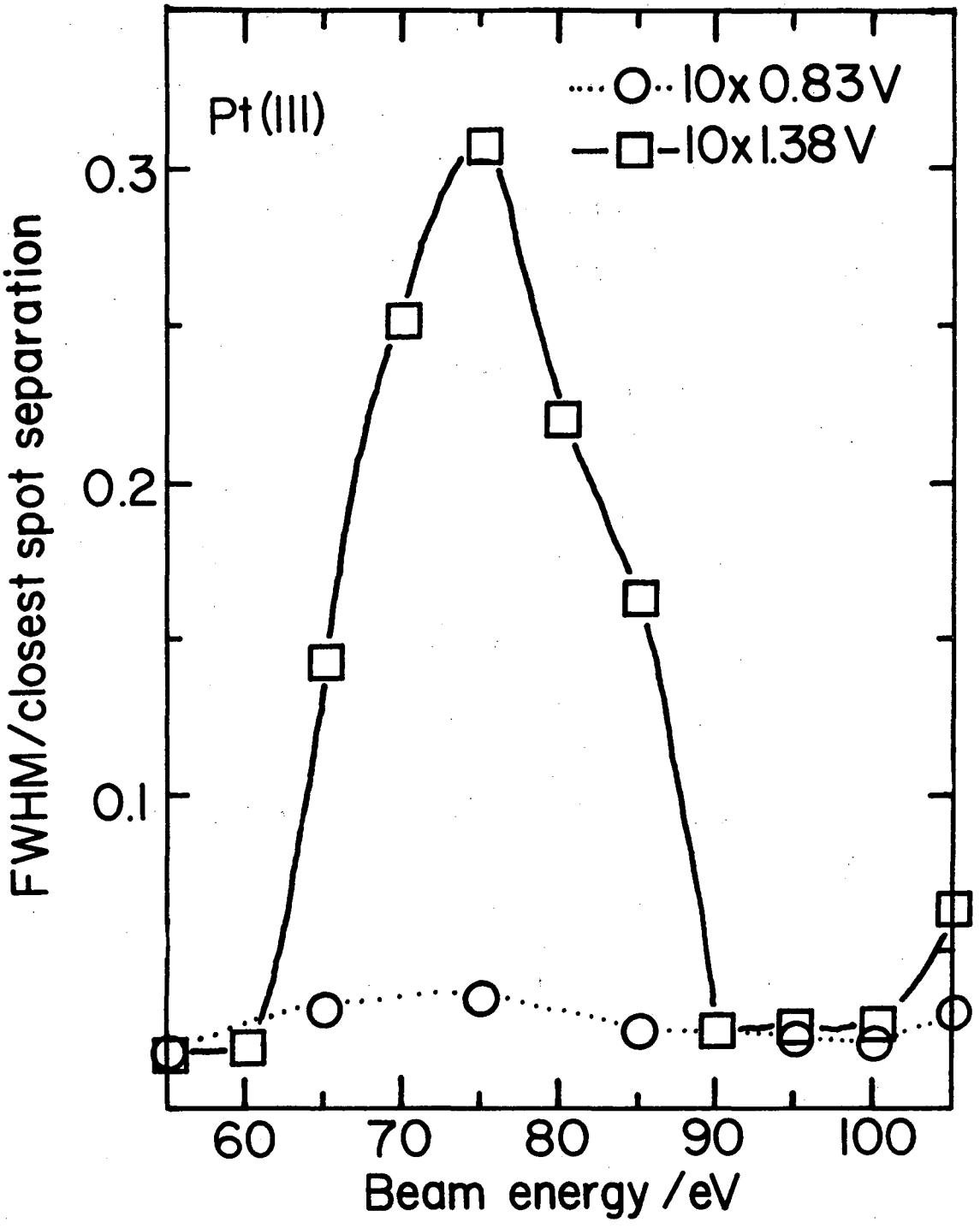

XBL 838-11292

Fig. 3

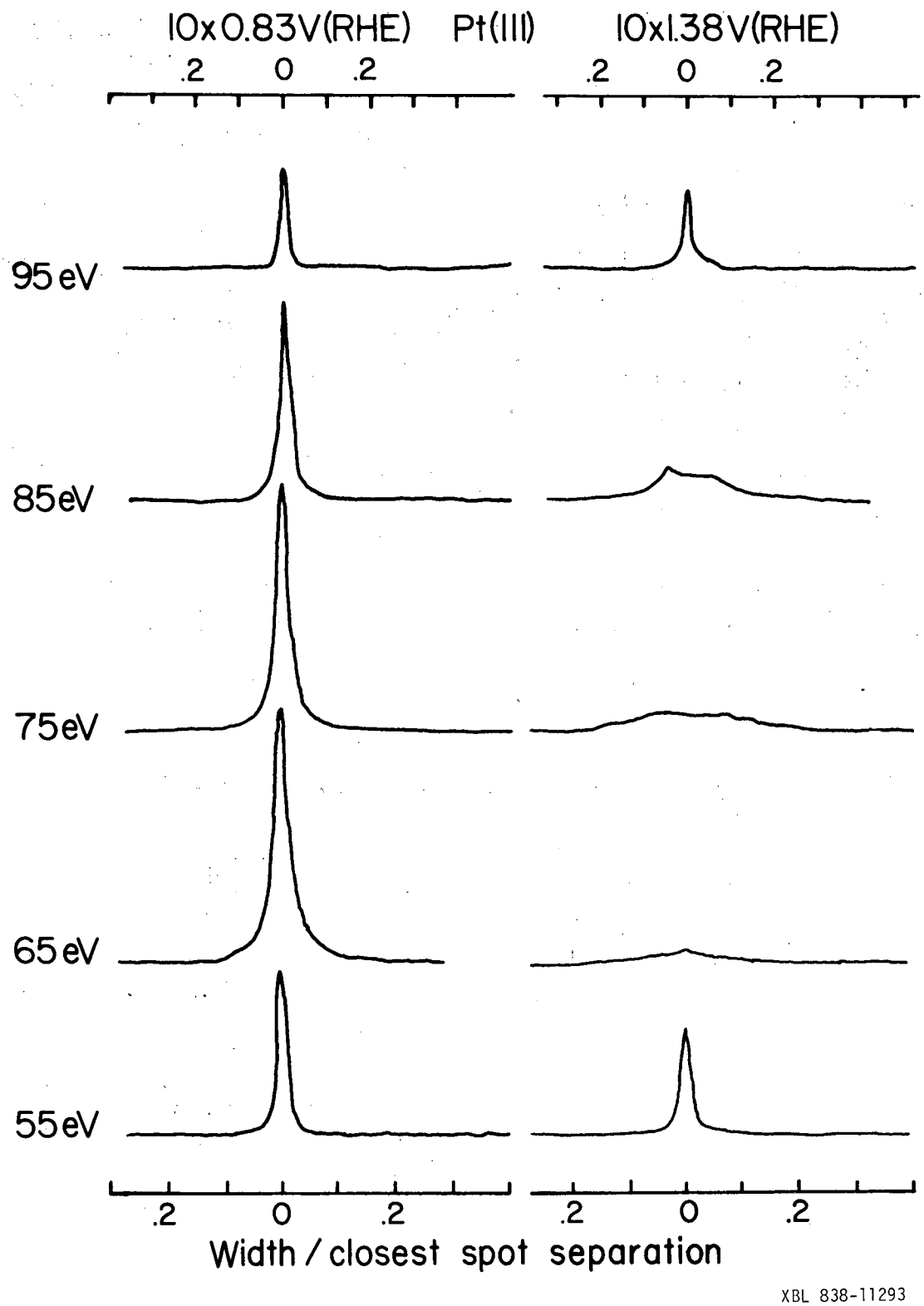

XBL 838-11293

Fig. 4

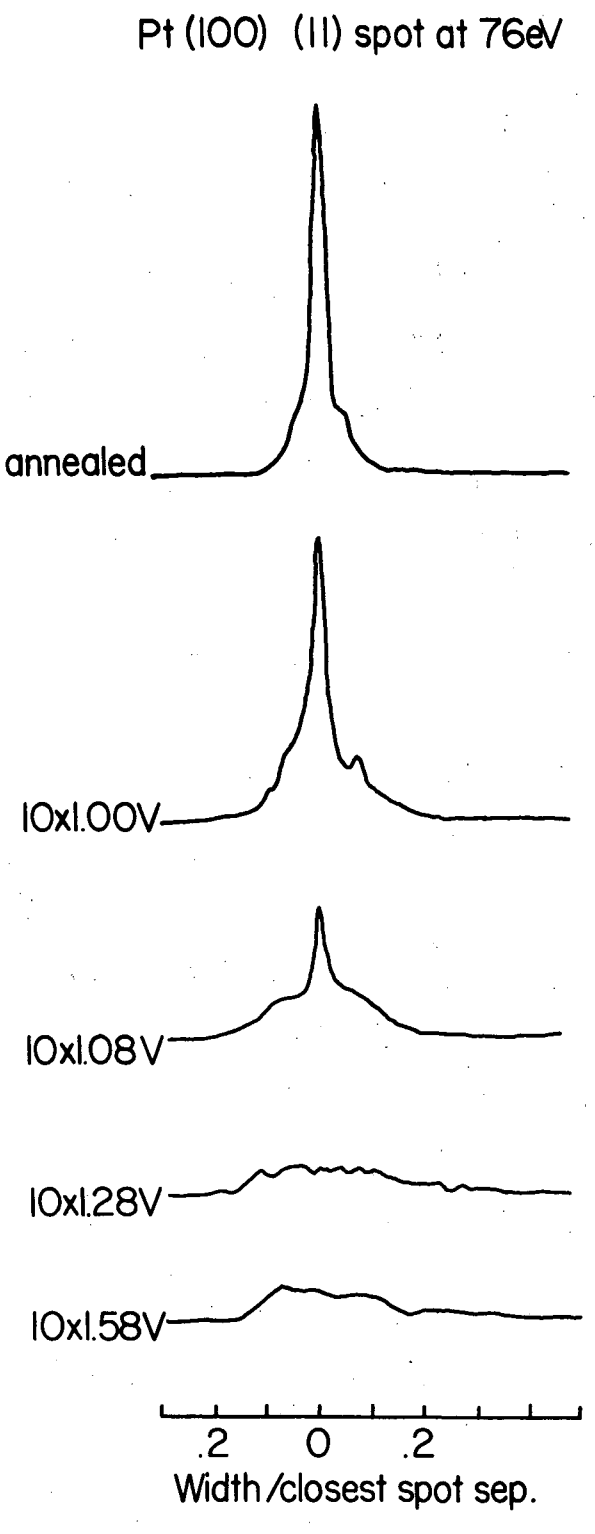
Pt (100) (11) spot at 76eV
annealed
10x1.00V
10x1.08V
10x1.28V
10x1.58V
.2
0
.2
Width/closest spot sep.
XBL 839-11326

Fig. 5

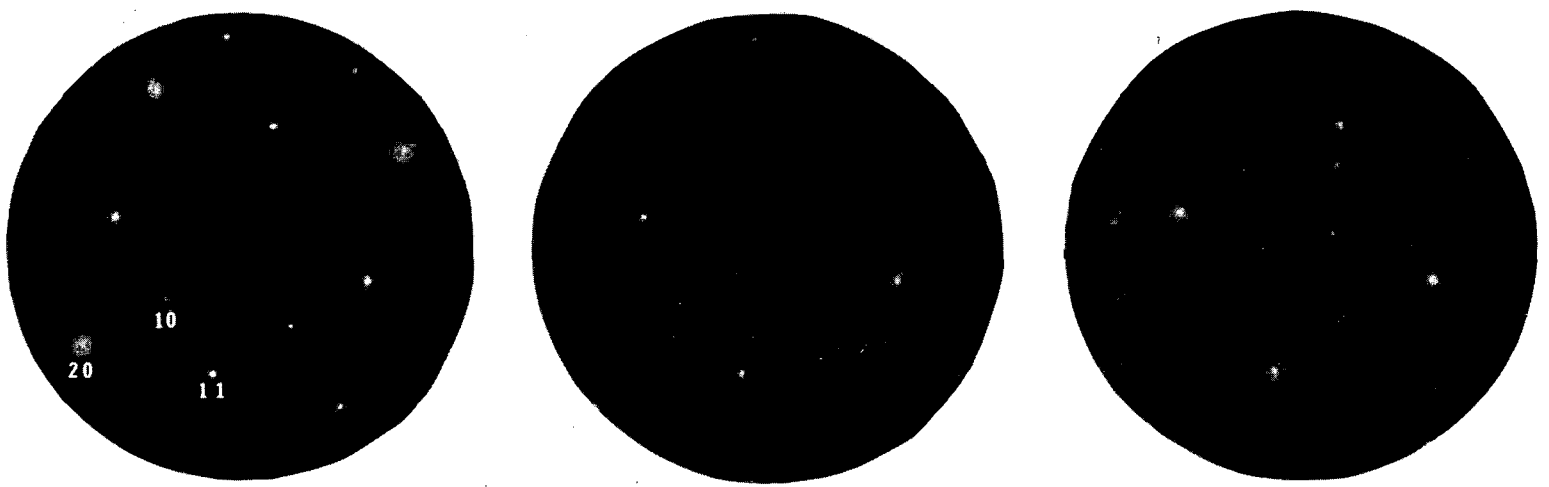
LEED at 176eV after ten cycles
10
20
11
to 1.08V (RHE)
to 1.28V (RHE)
to 1.58V (RHE)
XBB 837-6065

Fig. 6

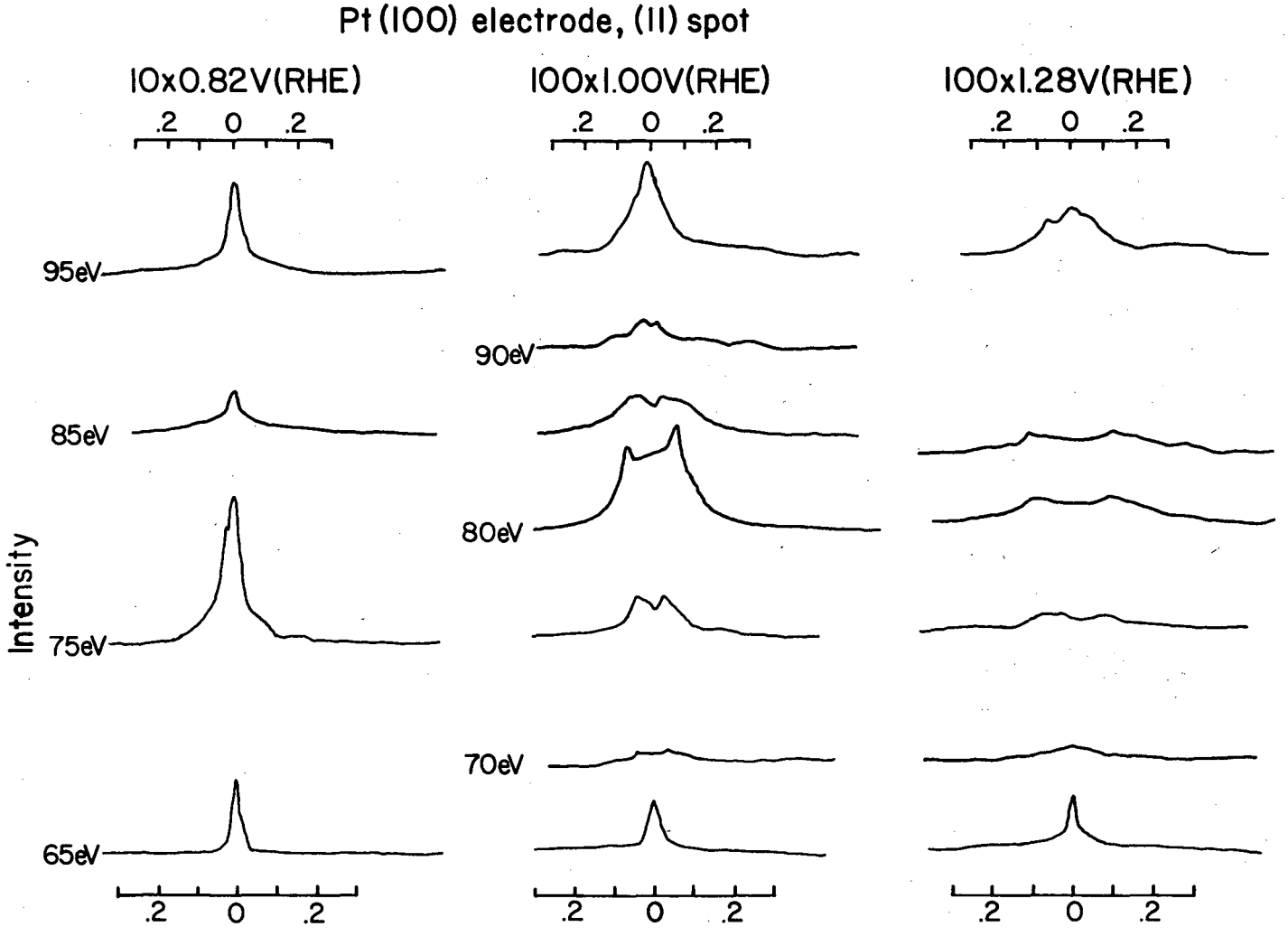

XBL 839-11325

Fig. 7

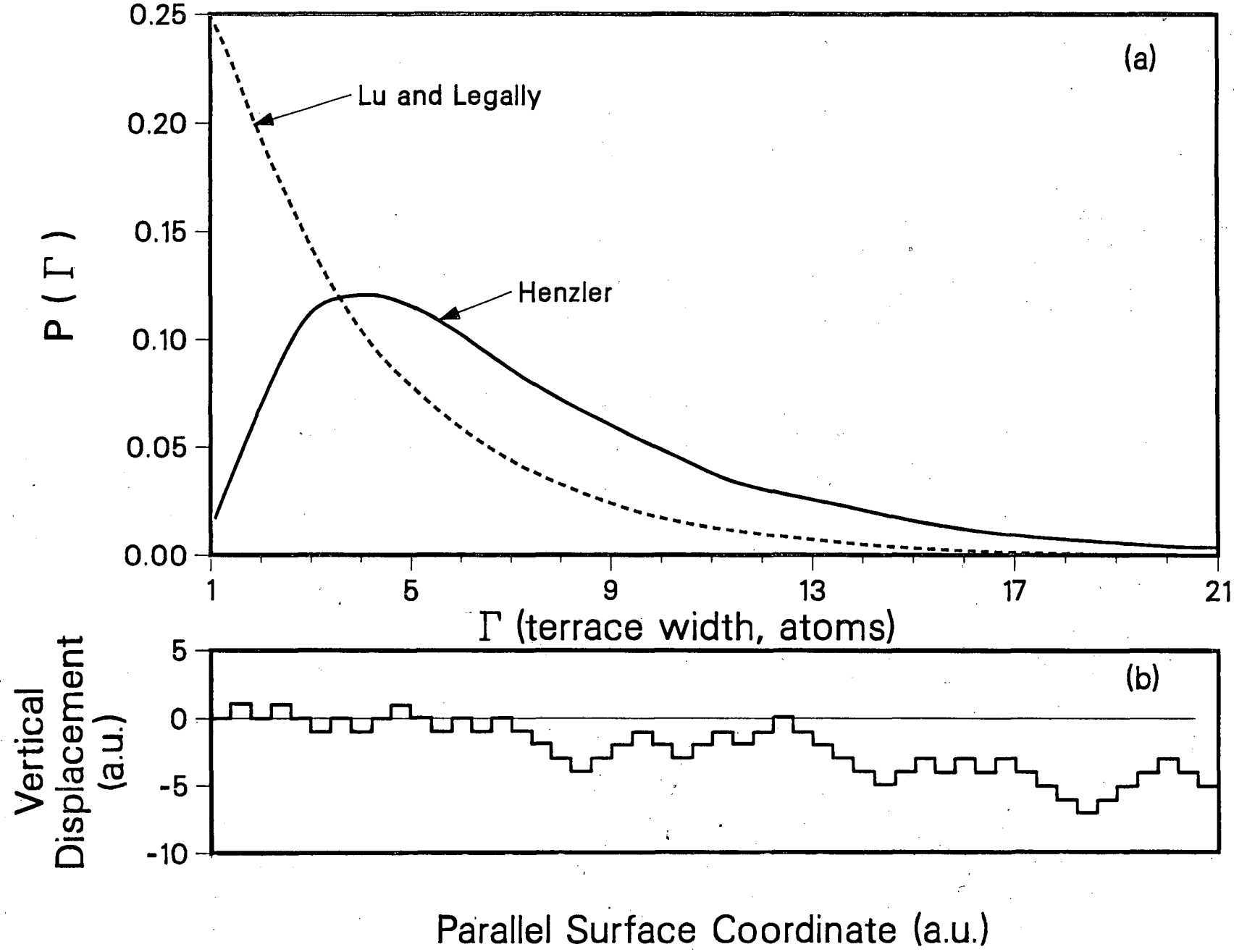

XCG 8410-13345

Fig. 8

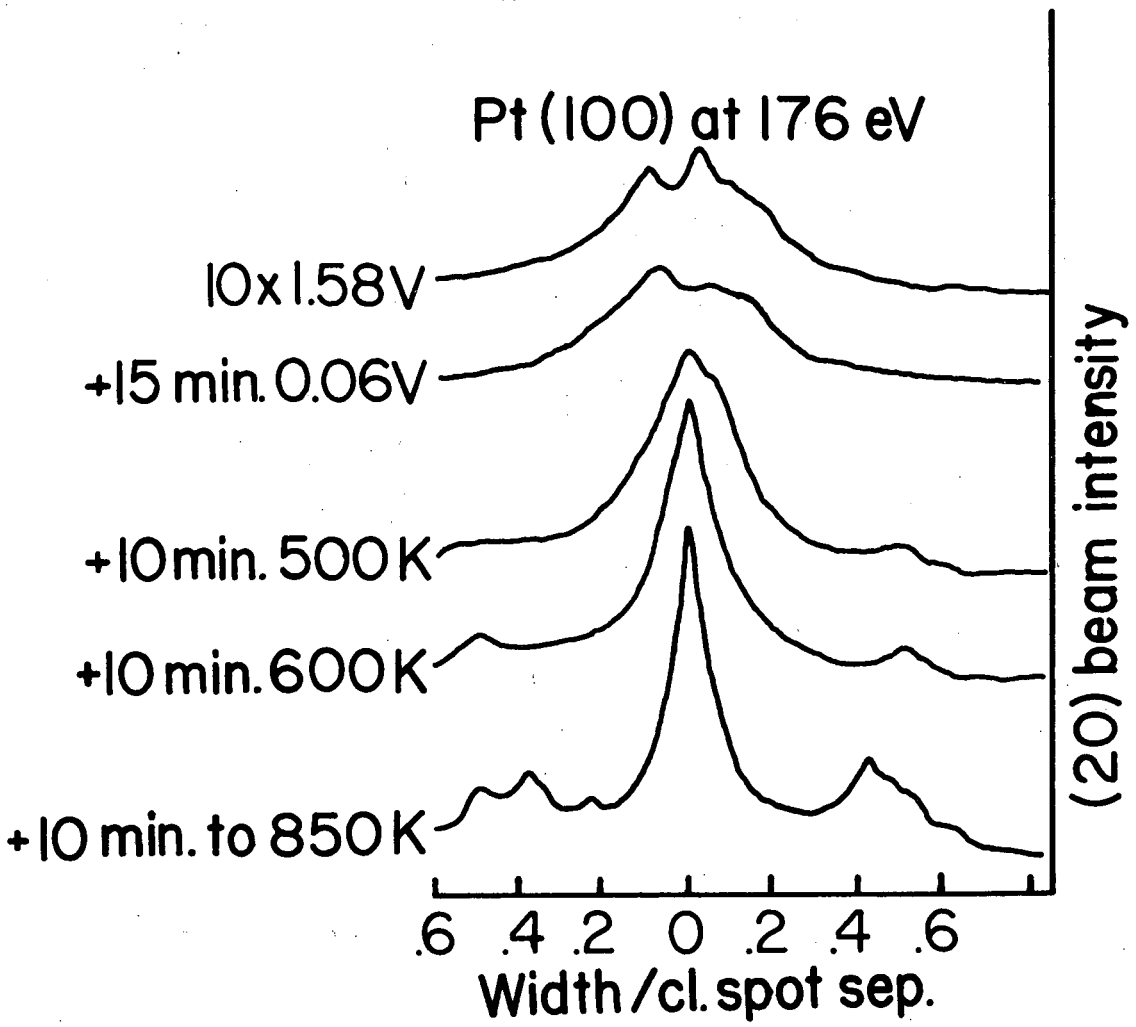

XBL 838-11291

Fig. 9

TECHNICAL INFORMATION DEPARTMENT
LAWRENCE BERKELEY LABORATORY
UNIVERSITY OF CALIFORNIA
BERKELEY, CALIFORNIA 94720